

## **Lead and copper-induced hormetic effect and toxicity mechanisms in lettuce (*Lactuca sativa* L.) grown in a contaminated soil**

**Jianhong Li<sup>a,b,#</sup>, Yong Qiu<sup>c,#</sup>, Qingjie Zhao<sup>b</sup>, Dongliang Chen<sup>d</sup>, Zhipeng Wu<sup>d</sup>, An-an Peng<sup>a</sup>, Nabeel Khan Niazi<sup>e,f</sup>, Lukáš Trakal<sup>g</sup>, Ruben Sakrabani<sup>h</sup>, Bin Gao<sup>i</sup>, Hailong Wang<sup>a,j,\*</sup>, Weidong Wu<sup>b,\*</sup>**

<sup>a</sup> Biochar Engineering Technology Research Center of Guangdong Province, School of Environmental and Chemical Engineering, Foshan University, Foshan, Guangdong 528000, China

<sup>b</sup> College of Tropical Crops, Hainan University, Haikou, Hainan 570228, China

<sup>c</sup> College of Oceanology and Food Science, Quanzhou Normal University, Quanzhou, Fujian 362000, China

<sup>d</sup> Institute of High Energy Physics, Chinese Academy of Sciences, Beijing 100039, China

<sup>e</sup> Institute of Soil and Environmental Sciences, University of Agriculture Faisalabad, Faisalabad 38040, Pakistan

<sup>f</sup> School of Civil Engineering and Surveying, University of Southern Queensland, Toowoomba 4350 Queensland, Australia

<sup>g</sup> Department of Environmental Geosciences, Faculty of Environmental Sciences, Czech University of Life Sciences Prague, Kamýcká 129, 16500, Praha 6, Suchbát, Czech Republic

<sup>h</sup> School of Water, Energy & Environment, Cranfield University, Cranfield, MK45 4DT Bedfordshire, United Kingdom

<sup>i</sup> Department of Agricultural and Biological Engineering, University of Florida, Gainesville, FL, USA

<sup>j</sup> Key Laboratory of Soil Contamination Bioremediation of Zhejiang Province, Zhejiang A&F University, Hangzhou, Zhejiang 311300, China

# Jianhong Li and Yong Qiu contributed equally to this work and should be considered co-first authors.

\* Corresponding authors. E-mail addresses: [hailong.wang@fosu.edu.cn](mailto:hailong.wang@fosu.edu.cn) (H. Wang), [wduw@hainanu.edu.cn](mailto:wduw@hainanu.edu.cn) (W. Wu).

## Abstract

Lead (Pb) and copper (Cu) contamination seriously threatens agricultural production and food safety. This study aims to investigate Pb and Cu induced hormetic effect and toxicity mechanisms in lettuce (*Lactuca sativa* L.) and establish reliable empirical models of potentially toxic elements (PTEs) transfer in the soil–plant system. The content and distribution of Pb and Cu at subcellular levels in lettuce plants were examined using inductively coupled plasma-mass spectrometry, differential centrifugation and micro-X-ray fluorescence spectroscopy. The PTE-loaded capacity of Pb that ensures food safety was lower than that of Cu in the studied soil, but the PTE-loaded capacity of Pb that limits yield was higher than that of Cu. Lead in lettuce roots mainly accumulated in the cell wall (41%), while Cu mainly accumulated in the vacuoles (46%). The Pb and Cu were primarily distributed in the radicle of lettuce seeds under severe PTE stress, resulting in no seed development. Iron plaque formed on the root surface of lettuce seedlings and sequestered Pb and Cu via chelation. At the same concentration, lettuce was less tolerant to Cu in contaminated soil than Pb due to the higher activity of Cu ions in the soil. Lead was more phytotoxic to lettuce than Cu, however, since the radicle emerged from the seed under severe Cu levels, while it did not protrude under severe Pb levels. The potentially damaging effect of Pb in the visually healthy lettuce appeared to be higher than that of Cu under the same soil contamination level.

**Keywords:** Potentially toxic element; soil contamination; PTE-loaded capacity; safe lettuce production;  $\mu$ -XRF

## Abbreviations

ICP-MS, inductively coupled plasma-mass spectrometry; PTE, potentially toxic element; PCEFS, PTE-loaded capacity that ensures food safety; PCLY, PTE-loaded capacity that limits yield; PCKS, PTE-loaded capacity that kills seed;  $\mu$ -XRF, micro X-ray fluorescence spectroscopy

## 1. Introduction

Contamination of soils with potentially toxic elements (PTEs) has led to severe environmental and health problems globally (Mackay et al., 2013; Cai et al., 2019; Fang et al., 2020). It has been reported that the local children in smelter-affected areas around a copper smelter in Hubei province, China were likely under high health risks, up to 30.25 times higher than the acceptable healthy level, and most of the health risks were resulted from PTEs exposure through ingestion of food crops (Cai et al., 2019). A further risk factor for PTEs is their higher toxicity in animals, including humans, than in plants (DEFRA, 2002). Therefore, studying the potential risk of PTEs in crops is vitally important in order to reduce the intake of PTEs.

Recent toxicology and risk assessment studies revealed PTE-induced hormesis in plants, i.e., stimulation in plant growth at low-doses while suppression at high-doses, which is called hormetic effect (Shahid et al., 2019). The biomass of plants can be increased by exposure to PTEs before reaching the threshold that would cause a negative effect (Yang et al., 2016; Shahid et al., 2019). It is assumed that human exposure to PTEs below the levels specified in official standards carries minimal human health risk (DEFRA, 2002). Since the concentration of PTEs in plants is not visibly discernible, humans may ingest potentially harmful levels of PTEs when consuming visually healthy plants (Ferri et al., 2015; Yuan et al., 2019; Bandara et al., 2020). Therefore, in order to protect consumers against elevated exposure to PTEs through the ingestion of visually healthy crops, PTE-induced hormetic effect for crops and their mechanisms, as well as information concerning the relationship between PTE contamination levels and safe food production, e.g., the exact PTE levels that meet food safety standards or lead to a decline in crop yields should be explored (e.g., Chen et al., 2020; Xia et al., 2020). Investigating the toxicity and accumulation of PTEs in crops and unraveling the tolerance mechanism of crops in soil-plant systems can help efforts to reduce the risk of PTE intake from visually healthy crops.

Mwamba et al. (2016) reported that the efficiency of different alleviation strategies could vary against various PTEs (with different elemental characteristics) toxicity to plants. The distribution of PTEs at subcellular level

could directly present the level of metal intra-cellular activity, thus the extent of potential toxicity to plant (van Assche and Clijsters, 1990). Determining the subcellular distribution of PTEs and their localization in plant tissues can provide helpful information on PTE tolerance of plants and toxicity mechanisms of PTE to plants (Sokolova et al., 2005; Wu et al., 2013; Sun et al., 2018). Synchrotron radiation-based X-ray fluorescence spectroscopy ( $\mu$ -XRF) and X-ray absorption fine structure (XAFS) spectroscopy are often used to demonstrate remediation effects on PTE pollution (Wu et al., 2017; Li et al., 2019a, b) and the accumulation mechanisms of PTEs in plants (Lu et al., 2017b). Some studies have revealed the translocation of PTEs in plants using differential centrifugation, inductively coupled plasma-mass spectrometry (ICP-MS) and  $\mu$ -XRF spectroscopy (Wu et al., 2013; Sun and Luo, 2018). The  $\mu$ -XRF method can be effectively used to visualize the distribution of mineral elements in micro-regions of plant organs (Lu et al., 2017b). Using  $\mu$ -XRF spectroscopy, Lu et al. (2017b) reported a clear preferential localization of copper (Cu) in the meristematic zone in the root tips of rice, compared with the elongation zone. In response to lead (Pb) and chromium (Cr) stress,  $\mu$ -XRF determined that Pb and Cr were mainly distributed in the cortex of the root of pak choi (*Brassica chinensis* L.), where they restrict transport from the root to the stem (Wu et al., 2013).

Lettuce (*Lactuca sativa* L.) is a PTEs-accumulating plant (Cobb et al., 2000) and is recommended for standard toxicity tests (e.g., ISO/CD 17126; ISO, 1995). Lettuce is one of the most consumed leafy vegetables (Kim et al., 2016). The lettuce grown in the United States alone has been valued at over 2.4 billion USD (NAAS, 2015). Lettuce is also widely cultivated in China, with a harvested area of 0.65 million hectares (51.1% of the world total) in 2018 (FAOSTAT, 2019). In addition, Cu is an essential element for plant functioning in normal conditions, using active and passive transport systems during uptake, whereas Pb is a highly toxic element without any known essential function in plants, using passive transport systems (e.g., the apoplastic pathway or via  $\text{Ca}^{2+}$ -permeable channels) during uptake (Trakal et al., 2013, 2015). Therefore, Pb and Cu are likely to present some specificity in

their induced hormetic effect and their toxicity mechanism in lettuce. Revealing the toxicity and transport mechanism of Pb (a representative toxic element) and Cu (a representative essential element) in lettuce using advanced techniques can show us a clearer knowledge on the health risks of different kind of PTEs via visually healthy lettuces intake. In the current study, differential centrifugation, ICP-MS, and  $\mu$ -XRF were utilized to investigate the toxicity and transport of Pb and Cu in lettuce under elevated Pb and Cu levels in the soil-plant system.

We hypothesized that Pb and Cu induced hormetic effect and toxicity mechanisms in lettuce are different due to the different elemental characteristics of Pb and Cu. This may result in different tolerance limits of Pb and Cu for food safety, the level that initiates a decrease in lettuce weight, and the level that indicates no seed development. The objectives of this study were to: (1) reveal Pb and Cu induced hormetic effect and toxicity to lettuce; (2) investigate the subcellular distribution of Pb and Cu in lettuce and its toxicity mechanism; and (3) explore the visual distribution of Pb and Cu in lettuce seeds and tissues as well as the toxicity and transport mechanism of Pb and Cu.

## **2. Materials and methods**

### *2.1. Pot experiment*

The pristine or PTEs-uncontaminated loam soil (at depths of 0–20 cm) was collected from Dareng Village (19.08°N, 109.06°E) in Changjiang County, Hainan Province, China. The soil was classified as Udic Ferralsol in accordance with the soil classification system of the Food and Agricultural Organization of the United Nations (with a soil texture of loam). The collected soil was amended with 2.3% (w/w) corn straw biochar and incubated for 3 months. The pH value of the resulting soil was 6.3, and its soil organic carbon and cation exchange capacity were 29.7 g kg<sup>-1</sup> and 94.2 mmol kg<sup>-1</sup>, respectively. The concentrations of total nitrogen, total phosphorus, and available potassium of the soil were 1.32, 0.46, and 0.41 g kg<sup>-1</sup>, respectively. The total Pb and Cu concentrations

of the soil were 55.3 mg kg<sup>-1</sup> and 9.51 mg kg<sup>-1</sup>, respectively.

The soil was air-dried, sieved (< 2 mm), and then stored in air-tight plastic bags prior to the pot experiment. To prepare the contaminated soil for the pot experiment, 2 kg of each mixed soil (dry weight) was placed into a plastic cask, and deionized water was then added to reach the 50% water holding capacity of the soil. The aim was to allow the Pb(NO<sub>3</sub>)<sub>2</sub> or Cu(NO<sub>3</sub>)<sub>2</sub> aqueous solutions to uniformly disperse into the soil. To achieve an elevated Pb and Cu stress in the studied soils, seven treatments with final Pb or Cu contents of 0, 25, 50, 250, 500, 2500, or 5000 mg kg<sup>-1</sup> were prepared separately. Specifically, the soil samples were spiked with 200 mL of 0, 1.206, 2.41, 12.06, 24.13, 120.6, or 241.3 mM Pb(NO<sub>3</sub>)<sub>2</sub> aqueous solution as well as 0, 3.93, 7.87, 39.3, 78.7, 393.4, or 786.8 mM Cu(NO<sub>3</sub>)<sub>2</sub> aqueous solution, respectively. Accordingly, the risk screening values of Pb and Cu for the new soil environmental quality standard of agricultural land in China (designated GB 15618–2018) under a soil pH of 5.5–6.5 were 100 mg kg<sup>-1</sup> and 50 mg kg<sup>-1</sup>, respectively. Contaminated soils were aged for 3 months and their moisture contents in casks were adjusted daily to maintain a constant 70% of the water holding capacity.

After incubation of the Pb and Cu contaminated soil, the soil samples were air-dried and weighed in a polyethylene pot (500 g pot<sup>-1</sup>) for the experiment. A detailed description of lettuce growth experiment is given in the Supporting Information (Text S1). The plants were harvested for analysis after 40 days of growth, when they had reached the mature stage and were ready to be consumed.

## *2.2. Separation and analysis of subcellular fractions*

Fresh lettuce plants were washed with deionized water and divided into shoots and roots. Next, 4.0 g of lettuce shoots and 3.0 g of lettuce roots from each treatment were weighed and homogenized in a medium with 20 mL of 250 mM sucrose, 1.0 mM dithioerythritol, and 50 mM Tris-HCl (at pH 7.5). The medium had been cooled to 4°C prior to the addition of homogenate. The homogenate was then filtered through a nylon cloth (80 μm), and the

residue was washed with 5 mL of the medium. The material collected on the nylon cloth (Wu et al., 2013) was adopted as the cell wall subcellular fraction (SV). Finally, the supernatant was separated according to Wu et al. (2013) into the plastid (SIV), nucleus (SIII), and mitochondrion (SII) fractions at 4°C using a refrigerated centrifuge (H2050R, Cence, China). The last supernatant was designated the soluble fraction (SI). All of the subcellular fractions of lettuce roots and shoots were freeze-dried and digested with a concentrated mixture of HNO<sub>3</sub> and H<sub>2</sub>O<sub>2</sub> (3 mL; 2:1 v/v) in a microwave digestion system (MDS-6, SINED, China). Lead and Cu concentrations were determined using inductively coupled plasma-mass spectrometry (X 7, Thermo Fisher, USA).

### *2.3. Analysis of plant and soil samples*

Before harvesting the lettuce, chlorophyll content was measured using a chlorophyll analyzer (SPAD-502 Plus, Konica Minolta, Japan). The chlorophyll content of the lettuce leaves on the 40th day of growth was measured 5 times for each pot. After harvesting, several lettuce plants were randomly selected from each pot and divided into shoots and roots. The shoots and roots were dried in an oven at 105°C for 30 minutes and 70°C for 48 hours. The dried plant samples were ground and sieved (< 0.5 mm), and 0.3 g of each sample was weighed in a polytetrafluoroethylene digestion tube. The samples were then digested with a concentrated solution of HNO<sub>3</sub> and H<sub>2</sub>O<sub>2</sub> (6 mL; 2:1 v/v) in a microwave digestion system.

In order to estimate the availability of the PTEs in the soil, 0.05 M ethylenediaminetetraacetic acid (EDTA) was used (Liu et al., 2017). Soil pH was measured with a pH meter, using a mixture of soil and deionized aqueous solution (w/v ratio, 1:2.5) that was shaken for 30 min. The 1 M ammonium acetate (pH 7.0) method was used to determine the cation exchange capacity as well as the levels of several exchangeable mineral elements (i.e., K, Ca, Mg, and Zn) in the soil (Rayment and Higginson, 1992). The K<sub>2</sub>Cr<sub>2</sub>O<sub>7</sub>-heating method based on Bao (2000) was chosen to measure the content of soil organic carbon. Total phosphorus (P<sub>tot</sub>), Pb, and Cu concentrations in the soil were determined according to an improved method based on Webb and Adeloju (2013) and Wu et al.

(2014). These concentrations were measured by digesting 0.1 g of soil samples (0.149 mm sieved) with 6 mL of solution (HNO<sub>3</sub>/H<sub>2</sub>O<sub>2</sub>/HF; 3/2/1 v/v/v) in a microwave digestion system (MDS-6, SINED, China). The temperature was maintained at 85°C for 3 min, 125°C for 6 min, and 150°C for 6 min. The soil total nitrogen (N<sub>tot</sub>) was determined using a multi N/C analyzer (multi N/C 2100, Analytik Jena AG, Germany).

Concentrations of Pb, Cu, and P in the digested solutions were measured using an ICP-MS. The translocation factor (TF) was used to evaluate the ability of plants to translocate Pb or Cu from the roots to the shoots using the following equation:

$$TF = 100\% \times C_{\text{shoot}}/C_{\text{root}},$$

where C refers to the concentration of PTE in tissues (mg kg<sup>-1</sup> DW), and shoot refers to stems and leaves (Wu et al., 2013).

#### 2.4. Micro-X-ray fluorescence ( $\mu$ -XRF) analysis

Thin longitudinal sections (50  $\mu$ m) of lettuce seeds and seedlings were prepared on the 5th day after sowing and placed on Kapton tape for  $\mu$ -XRF analysis. This was accomplished using the beamline 4W1B of the Beijing Synchrotron Radiation Facility (BSRF, China), which runs 2.5 GeV electron with a current ranging from 150 to 250 mA. A detailed description of sample collection and preparation is found in the Supporting Information (Text S2). The data reduction and processing were performed using PyMca software (Solé et al., 2007).

#### 2.5. Statistical analysis

Results were expressed on a dry weight basis (mean  $\pm$  standard deviation of 3 replicates per treatment). The plant weight, chlorophyll of leaves, and concentrations of Pb and Cu in the tissues and subcellular fractions of lettuce under different treatments were analyzed via ANOVA (with a 95.0% confidence level) according to Tukey's multiple-range tests ( $p < 0.05$ ). Statistical analysis was carried out using SAS 9.1 software (SAS Institute, Inc., USA), and the figures were designed using Origin 8.0 software (Origin Lab, USA).



### 1 3. Results

#### 2 3.1. Growth of lettuce and its PTEs content under elevated Pb and Cu stress

3 The photos and detailed descriptions of lettuce growth status during the seedling period (the 5th day after  
4 sowing) and the harvest period (the 40th day) under Pb and Cu stress are shown in Fig. S1 and Text S3 of the  
5 Supporting Information, respectively. There was a significant ( $p < 0.05$ ) increase in the fresh weight of lettuce  
6 plants (yield) and the chlorophyll of leaves (SPAD value) at Cu concentrations of 250 mg kg<sup>-1</sup> when compared to  
7 the control treatment, while only significant increase in SPAD value at the same Pb level (Fig. 1). Lettuce fresh  
8 weight significantly decreased from 28.3 to 2.62 g pot<sup>-1</sup> and the chlorophyll of leaves decreased from 26.7 to 18.0  
9 with the increase in Cu level from 250 to 500 mg kg<sup>-1</sup>. The chlorophyll of leaves (SPAD) was significantly reduced  
10 from 25.9 to 22.9 and lettuce fresh weight was significantly reduced from 24.3 to 2.83 g pot<sup>-1</sup> with the increase  
11 in Pb level from 500 to 2500 mg kg<sup>-1</sup> (Fig. 1; Table S1). Therefore, a dose response phenomenon characterized  
12 by low-dose stimulation and high-dose inhibition was observed in the lettuce pot experiment under Pb and Cu  
13 stress, as shown in the “I,” “II,” “III,” and “IV” regions of Fig. 1.

14 The Pb toxicity in lettuce appeared at higher concentrations (i.e., 2500 mg kg<sup>-1</sup>) than Cu toxicity (i.e., 500 mg  
15 kg<sup>-1</sup>) as Pb and Cu levels were increased in the soil (Fig. 1; Figs. S1C, D). The response curve of lettuce fresh  
16 weight to the total PTE content in the studied soil under elevated Pb and Cu stress can be well expressed via a  
17 quadratic polynomial model, as shown in Figs. 2a, b. The fitted models were demonstrated by plotting the  
18 measured weight of lettuce plants under Pb and Cu stress against the corresponding calculated values (Figs. S2A,  
19 B). The results revealed that the lettuce yield began to decrease when Pb and Cu contents in the studied soil  
20 reached 997.2 mg kg<sup>-1</sup> and 212.1 mg kg<sup>-1</sup>, respectively (points A and C in Figs. 2a, b). Moreover, Pb and Cu  
21 contents in the soil were 2643.5 mg kg<sup>-1</sup> and 525.4 mg kg<sup>-1</sup>, respectively, when the lettuce yield decreased to 0 g  
22 pot<sup>-1</sup> (points B and D in Figs. 2a, b).

23 In terms of food safety policy, the tolerance limits for Pb and Cu in fresh leafy vegetables in China are 0.30  
24 mg kg<sup>-1</sup> (GB 2762–2017) and 10 mg kg<sup>-1</sup> (GB 15199–94), respectively. Concentrations of Pb and Cu in fresh  
25 lettuce shoots at the Pb level of 25 mg kg<sup>-1</sup> and the Cu level of 50 mg kg<sup>-1</sup> were 0.28 and 8.54 mg kg<sup>-1</sup>, respectively  
26 (Table S2); these values are below the tolerance limits in China. The changes in Pb and Cu concentrations in  
27 lettuce with increasing concentrations of total Pb and Cu in the studied soil can be modeled well via Equations (1)  
28 and (2):

$$29 \quad y = a + bx, \quad (1)$$

$$30 \quad y = e - c \cdot d^x, \quad (2)$$

31 where a, b, c, d and e are constants of the fitting equations.

32 The fitted models were found to be reliable (Figs. S2C, D). To reach the tolerance limits of Pb and Cu for leafy  
33 vegetables in China, we calculated that the total Pb and Cu concentrations of the studied soil would need to be  
34 65.1 and 89.9 mg kg<sup>-1</sup>, respectively (points E and F in Figs. 2c, d).

### 35 3.2. Availability of Pb, Cu, and other mineral elements in the soil

36 The EDTA-extractable Pb and Cu content in the studied soil before lettuce sowing increased with increasing  
37 Pb and Cu contamination levels (Table S3). A quadratic polynomial equation could well describe EDTA-  
38 extractable Pb and Cu contents under different levels (Fig. S3). Although EDTA-extractable Pb content was higher  
39 than that of Cu in the studied soil at the same contamination level, EDTA-extractable Pb ion content was  
40 significantly lower than Cu ion content (Table S3). The EDTA-extractable Pb ion content (0.06 mmol kg<sup>-1</sup> under  
41 a soil Pb concentration of 65.1 mg kg<sup>-1</sup>) was lower than Cu (0.53 mmol kg<sup>-1</sup> under a soil Cu concentration of 89.9  
42 mg kg<sup>-1</sup>) at the food safety threshold value (points E and G in Fig. S3). However, the EDTA-extractable Pb ion  
43 content (3.53 mmol kg<sup>-1</sup> under a Pb concentration of 997 mg kg<sup>-1</sup>) was higher than Cu (1.37 mmol kg<sup>-1</sup> under a  
44 Cu concentration of 212 mg kg<sup>-1</sup>) when the lettuce yield began to decrease (points F and G in Fig. S3). The

45 exchangeable K, Ca, Mg, and Zn in the studied soil increased with increasing Pb and Cu contamination levels,  
46 while the pH values significantly decreased with increasing PTEs levels (Table S4).

### 47 *3.3. Distribution of Pb and Cu in plant tissue*

48 Lead and Cu concentrations in each shoot and root tissue increased significantly ( $p < 0.05$ ) with increasing Pb  
49 and Cu levels in the soil (Table 1 and Fig. S4), with the exception of those at the Pb level of 25 mg kg<sup>-1</sup> ( $p > 0.05$ ).  
50 Before the lettuce was seriously poisoned, the maximum Pb and Cu concentrations in the shoots were 433 and  
51 300 mg kg<sup>-1</sup> dry weight (DW), respectively, while the maximum Pb and Cu concentrations in the roots were 1789  
52 and 2353 mg kg<sup>-1</sup> DW, respectively (Table 1). Copper concentrations in the lettuce tissues were higher than Pb  
53 concentrations at the same contamination levels. The Pb translocation factors (33.1%–23.6%) from the roots to  
54 the shoots slowly decreased with increasing Pb levels (Fig. S5). The Cu translocation factors (65.5%–12.7%),  
55 however, sharply decreased with increasing Cu levels (Fig. S5).

### 56 *3.4. Subcellular distribution of Pb and Cu in plants*

57 The Pb and Cu concentrations in the different subcellular fractions of lettuce increased with increasing Pb and  
58 Cu levels in the soil (Table S2). As the Pb level increased from 0 to 500 mg kg<sup>-1</sup>, the Pb concentrations in the  
59 supernatant soluble fraction, mitochondrion, nucleus, plastid, and cell wall fractions of the lettuce respectively  
60 increased by 132-, 63.3-, 37.8-, 85.6-, and 47.4-fold in shoots and 170-, 30.3-, 31.3-, 64.5-, and 103-fold in roots  
61 compared to the control. When exposed to 250 mg kg<sup>-1</sup> of Cu, the Cu concentration in the soluble fraction,  
62 mitochondrion, nucleus, plastid, and cell wall fractions of the lettuce respectively increased by 3.1-, 5-, 10-, 3.4-,  
63 and 3.9-fold in shoots and 27.8-, 9.9-, 9.6-, 9.2-, and 23.6-fold in roots compared to the control.

64 Moreover, the percentage of Pb in the soluble fraction increased from 29.4 to 50.7% in the shoots. As the Pb  
65 level increased from 0 to 500 mg kg<sup>-1</sup>, the percentages of Pb in the mitochondrion, nucleus, and cell wall fractions  
66 decreased from 17.6% to 14.6%, 23.5% to 11.6%, and 20% to 12.4%, respectively (Fig. 3A). In the roots, as the

67 Pb level increased from 0 to 500 mg kg<sup>-1</sup>, the percentages of Pb in the soluble fraction and cell wall fraction  
68 increased from 22.5% to 37.9% and 23% to 41%, respectively (Fig. 3B). In contrast, the percentages of Pb in the  
69 mitochondrion, nucleus, and plastid fractions in the roots were significantly reduced.

70 As the Cu level increased from 0 to 250 mg kg<sup>-1</sup>, the percentage of Cu in the soluble fraction of shoots (Fig.  
71 3C) decreased from 51.4% to 42%, while the percentages of Cu in the mitochondrion and nucleus fractions  
72 increased slightly from 8.3% to 11% and 3.9% to 10.7%, respectively. When the Cu level increased from 0 to 250  
73 mg kg<sup>-1</sup>, the percentages of Cu in the soluble fraction and cell wall fraction of plant roots increased from 32.4%  
74 to 46.1% and 29% to 35.1%, respectively (Fig. 3D). The percentages of Cu in the nucleus, plastid, and  
75 mitochondrion fractions were slightly decreased, however.

### 76 *3.5. Distribution of Pb, Cu, and other elements in longitudinal sections of lettuce seeds and seedlings*

77 The distribution patterns of different elements in the longitudinal sections, as well as photos of seeds and  
78 seedlings under different Pb and Cu levels, are shown in Figs. 4–7. The Pb intensities over the entire longitudinal  
79 section of lettuce seeds under severe Pb levels (5000 mg kg<sup>-1</sup>; Fig. 4B) indicate that Pb was mainly distributed on  
80 the hypocotyl side (including the hypocotyl, shoot apex, and root apex) of seeds (region “a” in Fig. 4). In the  
81 cotyledon side region (including the cotyledons, endosperm, and seed coat) of seeds (region “b” in Fig. 4), Pb  
82 exhibited a more constrained distribution (Fig. 4B). Higher intensities of Mn, Fe, and Zn (Figs. 4E, F, H) were  
83 detected on the hypocotyl side (region “a”). However, K and Ca (Figs. 4C, D) exhibited higher intensities on both  
84 the hypocotyl side and cotyledon side of lettuce seeds. According to the Pearson correlation coefficient (Table S5),  
85 Pb was significantly correlated with other elements (R = 0.839\*\* for Fe, 0.624\*\* for Ca, and 0.603\*\* for Mn) in  
86 lettuce seeds. The high Cu concentrations were distributed over almost the entire seed under severe Cu levels  
87 (2500 mg kg<sup>-1</sup>), although higher Cu concentrations were found on both the hypocotyl side (region “c” in Fig. 5B)  
88 and the cotyledon side (region “d” in Fig. 5) of lettuce seeds. Similarly, high intensities of K, Ca, Mn, Fe, and Zn

89 (Figs. 5C–G) were observed on the tops of the hypocotyl and cotyledon sides of lettuce seeds. Copper was  
90 significantly correlated with other elements ( $R = 0.874^{**}$  for Mn,  $0.663^{**}$  for Fe, and  $0.337^{**}$  for Ca) in lettuce  
91 seeds (Table S5).

92 High concentrations of K, Ca, Mn, Fe, Cu, and Zn (Figs. 6C–H) and low concentrations of Pb (Fig. 6B)  
93 accumulated in both the upper half (i.e., shoots) and lower half (i.e., roots) of lettuce seedlings (Fig. 6A) under Pb  
94 stress ( $50 \text{ mg kg}^{-1}$ ). In the longitudinal section of shoots (Fig. 7a) of lettuce seedling under Cu stress ( $50 \text{ mg kg}^{-1}$ ),  
95 high K, Ca, Cu, Mn, Fe, and Zn (Figs. 7a B–G) contents were found in the stem area (region “e” in Fig. 7a) and  
96 at the leaf edge. Weak intensities of Pb (Fig. 7a H) were detected in the shoots of lettuce seedling under Cu stress.  
97 In lettuce seedling roots (Fig. 7b) under Cu stress ( $50 \text{ mg kg}^{-1}$ ), high intensities of K, Ca, and Zn (Figs. 7b C, D,  
98 G) were found in both the root hair zone (region “f” in Fig. 7b) and the stem area, while high intensities of Cu,  
99 Mn, and Fe (Figs. 7b B, E, F) were mainly detected in the root hair zone. Weak intensities of Pb (Fig. 7b H) were  
100 also observed in the young root hair zone and the young stems of lettuce seedlings under Cu stress. The distribution  
101 between Cu and Fe ( $R = 0.766^{**}$  for Fe) was significantly related (Table S5).

## 102 4. Discussion

### 103 4.1. Lead and copper-induced hormetic effect and toxicity to lettuce

104 The increased lettuce yield and leaf chlorophyll in response to low concentrations of PTEs (i.e., Pb and Cu)  
105 in regions “I,” “II,” “III,” and “IV” (Fig. 1) and the inhibition at high concentrations, indicate a hormetic effect  
106 (Shahid et al., 2017). The hormetic effect, a dose-response phenomenon characterized by low-dose stimulation  
107 and high-dose inhibition (Shahid et al., 2019), is commonly found in toxicological evaluations of biomedical  
108 applications (Calabrese, 2008; Shahid et al., 2019). A marked hormetic effect was found in a cultivation  
109 experiment of *Jatropha curcas* L. cuttings under soil Pb-stress (Shu et al., 2012). Shu et al. (2012) discovered that  
110 the leaf area as well as the chlorophyll a and b contents in cuttings all peaked at Pb levels of  $100 \text{ mg kg}^{-1}$ . Similarly,

111 the root biomass of carrot attains the highest value at a Cu level of 200 mg kg<sup>-1</sup> (Hou et al., 2018).

112 The lettuce, grow in the studied soil at Pb or Cu level of 250 mg kg<sup>-1</sup>, might be regarded as visually healthy  
113 vegetable by people since the lettuce yield and leaf chlorophyll of these lettuce plants was higher than that of  
114 lettuce in the control treatment. The content of Pb (6.33 mg kg<sup>-1</sup>) and Cu (12.1 mg kg<sup>-1</sup>) in lettuce shoots, however,  
115 was 21.1- and 1.2-fold the tolerance limit for Pb (0.30 mg kg<sup>-1</sup>) and Cu (10 mg kg<sup>-1</sup>) in fresh leafy vegetables in  
116 China, where the significantly higher limit for Cu is caused due to its nutrient essentiality. Yuan et al. (2019)  
117 reported that long-term consumption of polluted vegetables (with PTEs exceeded the contamination limitations  
118 for food in China) grown in PTE-contaminated soils, especially cabbage and lettuce, are likely to increase  
119 carcinogenic and non-carcinogenic health risks. Thus, the health risk of Pb in the visually healthy lettuce was  
120 much higher than that of Cu under the same soil contamination level.

121 In addition, our results revealed that the increase in yield and leaf chlorophyll of lettuce occurred over a larger  
122 range of Pb concentrations than Cu concentrations (Fig. 1). This may be primarily attributed to the higher  
123 extractable ion content of Cu than Pb in contaminated soil under the same severe PTE level. Thus, more damaging  
124 Cu ions would be taken up by lettuce plants than Pb ions. The excessively absorbed Cu and Pb ions may also  
125 interfere with various structural, physiological, and biochemical aspects of lettuce processes, thereby inhibiting  
126 the growth of the plant and sometimes resulting in plant death (Setia et al., 2018). Moreover, the toxicity of Pb  
127 and Cu also significantly affects the chlorophyll content in lettuce under severe PTE levels (Fig. 1), which inhibits  
128 plant growth (Ali et al., 2015). The mineral nutrients, e.g., K, Ca, Mg, and Zn, in soil that are exchanged and  
129 released by Pb<sup>2+</sup> and Cu<sup>2+</sup> (Table S4) under Pb (less than 2500 mg kg<sup>-1</sup>) and Cu level (less than 500 mg kg<sup>-1</sup>) may  
130 contribute to the hormetic effect of biomass and chlorophyll (SPAD) in lettuce.

131 The PTEs concentrations in lettuce plants reach 3 levels after the PTEs absorption: the tolerance limit of PTEs  
132 for food safety, the level that initiates a decrease in lettuce weight, and the level that results in lettuce seed mortality.

133 Based on the fitted models (Figs. 2, S2 and Text S4), we suggest that the total Pb and Cu concentrations in the  
134 studied soil are 65.1 and 89.9 mg kg<sup>-1</sup>, 997.2 and 212.1 mg kg<sup>-1</sup>, and 2643.5 and 525.4 mg kg<sup>-1</sup> for the 3 PTE-  
135 loaded capacities of soil for growing lettuce, respectively, i.e., the PTE-loaded capacity that ensures food safety  
136 (PCEFS), the PTE-loaded capacity that limits yield (PCLY), and the PTE-loaded capacity that kills seeds (PCKS).

137 The Pb concentration for the PCEFS in the studied soil was lower than 100 mg kg<sup>-1</sup>, which is the risk screening  
138 value for soil contamination of agricultural land at pH levels of 5.5–6.5 in China (GB 15618–2018). However,  
139 the Cu concentration for the PCEFS in the studied soil was higher than 50 mg kg<sup>-1</sup>, which is the risk screening  
140 value of Cu in China (GB 15618–2018). The Pb concentrations for the PCLY and PCKS in soil were nearly 2-  
141 and 5-fold the 500 mg kg<sup>-1</sup> risk intervention value for soil contamination of agricultural land at pH levels of  
142 5.5–6.5 in China, respectively (GB 15618–2018). There is no risk intervention value of Cu in China. Nevertheless,  
143 the Cu concentrations for the PCLY and PCKS in the studied soil were approximately 4- and 10-fold the risk  
144 screening value of Cu in China (50 mg kg<sup>-1</sup>), respectively (GB 15618–2018).

145 The food safety threshold and environmental lethal threshold of PTEs have been studied by several researchers  
146 (Ferri et al., 2015; Ding et al., 2015; Gomes et al., 2013). It assumes that when a certain study soil is chosen, the  
147 soil will have a specific capacity to load a PTE, since the elemental physicochemical properties of the soil are  
148 specific. Therefore, the PCEFS, PCLY, and PCKS values of a PTE for a particular crop in the study soil are also  
149 definite. This means that these PTEs capacities for a crop can be used to indirectly assess the contamination degree  
150 of the cultivated soil.

151 The PCLY and PCKS values of Cu in the studied soil were far lower than those of Pb. This might be related  
152 to concentration of bioavailable Pb and Cu in the soil, the toxicity of Pb and Cu to lettuce as well as the capacity  
153 of the plant for Pb and Cu uptake. Copper is an essential element for plants; in contrast, Pb is an unnecessary  
154 element (Gruszecka-Kosowska, 2019). Consequently, Cu is largely taken up and transported by plants, while Pb

155 is mainly excluded by plants or accumulates in their roots (Table 1). Generally, a particular crop displays different  
156 tolerances to different kinds of PTEs (Hou et al., 2018).

157 Soil properties, such as pH, cation exchange capacity, and organic matter, exert significant impacts on the  
158 content of available PTEs, i.e., the primary fraction of the PTEs uptake of plants from contaminated soils that  
159 affects the PTEs thresholds of plants in different soils (Ding et al., 2015; Wenzel, 2009). Our results indicated that  
160 the tolerance of lettuce to Pb and Cu was mainly affected by EDTA-extractable Pb and Cu ion content in the  
161 studied soil (Table S3 and Fig. S3). Soil pH values were significantly correlated with extractable PTEs contents  
162 in contaminated soil (Lu et al., 2017a). The higher the PTEs level in the contaminated soil, the lower the soil pH  
163 value (Table S4), which may contribute to the higher EDTA-extractable Pb and Cu in the soils under severe PTEs  
164 levels (Table S3). Moreover, available Pb exhibited a good correlation with Pb content in plants in contaminated  
165 soils (Ding et al., 2015). The lettuce plants could take up more extractable Pb and Cu ions in the contaminated  
166 soils under severe PTE levels until serious root damage occurred.

#### 167 *4.2. Distribution and translocation factor of Pb and Cu in plant tissues*

168 The translocation factor (TF) of Cu in lettuce decreased significantly (from 65% to 13%) with increasing Cu  
169 levels, whereas the TF of Pb was maintained at a low level (23%–33%) under different Pb levels (Table 1). This  
170 might be related to the different absorption and transport mechanisms of Pb and Cu in lettuce. To our knowledge,  
171 soil water with dissolved PTEs can enter up to the parenchyma via the apoplast or enter into the cells via the  
172 symplast during the PTEs uptake of plant roots (Trakal et al., 2015). Once in the endodermis, the Casparian strip  
173 forces all of the water and PTEs to follow the intracellular pathway (across the plasma membrane) using the active  
174 or passive transport systems (Trakal et al., 2015).

175 Copper uptake in root cells is passed through the symplast via active and passive transport, while Pb uptake  
176 is passed by the apoplastic pathway or via  $\text{Ca}^{2+}$ -permeable channels (i.e., passive transport; Trakal et al., 2015).



177 The cell membranes of plants contain proteins known as “proton pumps” that regulate the flow of Cu ions into  
178 cells (Himmelblau and Amasino, 2000). After Cu-uptake into the cell, copper chaperones (involved in intracellular  
179 transport) sequester Cu in a non-reactive form and interact with other transport proteins to transport Cu to the sites  
180 where plant metabolism is needed (Himmelblau and Amasino, 2000). Therefore, Cu could easily be transported into  
181 lettuce shoots under a suitable Cu level.

182 Kabata-Pendias (2011), however, reported that all of the elements are taken up passively when their  
183 concentrations exceed a threshold value, a situation that occurs in contaminated soils with high concentrations of  
184 PTEs. This means that under severe Cu levels, Cu would be forced to pass through a passive transport pathway  
185 into cells, making it more difficult to transport Cu into shoots (Trakal et al., 2013). Lead ions only move via  
186 passive transport systems (Trakal et al., 2013), exhibiting a low translocation factor in lettuce. Overall,  
187 accumulating PTEs (i.e., Pb and Cu) in the root tissues is a primary tolerance strategy in King 118 lettuce (*Lactuca*  
188 *sativa* L.) in response to elevated levels of PTEs. Moreover, the resistance to transfer in lettuce was higher for Cu  
189 than it was for Pb.

#### 190 4.3. Subcellular distribution of Pb and Cu in lettuce

191 Although the absolute concentrations of Pb and Cu in each subcellular structure of lettuce roots increased  
192 significantly with increasing Pb and Cu levels, the relative contents (percentages) of Pb and Cu increased  
193 dramatically only in the cell wall and soluble fraction (Table S2). Approximately 80% of Pb and Cu in the roots  
194 accumulated in the cell wall and soluble fraction. This was consistent with the subcellular proportions of Pb (76%)  
195 in the cell wall and soluble fractions of pak choi roots at a Pb level of 200 mg L<sup>-1</sup> and the proportion of Cu (86%)  
196 in the cell wall and soluble fractions of tomato seedling roots at a Cu level of 3.2 mg L<sup>-1</sup> (Dong et al., 2013; Wu  
197 et al., 2013). A possible accumulation mechanism for Pb and Cu in roots is chelation via binding sites in the root  
198 cell walls (Trakal et al., 2015). Excessive Pb and Cu are then sequestered mostly by vacuoles within the cells

199 when passing through the plasma membrane in order to protect organelles from their toxicity (Megateli et al.,  
200 2009; Wu et al., 2013; Sun and Luo, 2018).

201 Surprisingly, under elevated PTE stress, Pb exhibited a sharp tendency to be sequestered in the soluble fraction  
202 of lettuce shoots; Cu, however, presented a slight tendency to be accumulated in organelles and nuclei (Fig. 3).  
203 Consistent with our results, Cu also tended to be accumulated in the chloroplasts and nuclei of *Brassica napus*  
204 leaves (cultivars Zheda 622) when Cu stress increased from 3.2 to 12.8 mg L<sup>-1</sup> (Mwamba et al., 2016). A possible  
205 reason for this pattern is that high Cu stress easily induces significant harm to the architecture of thylakoid  
206 membranes in chloroplasts and nucleic acid in the nucleus, after which it accumulates in these cellular structures  
207 (Mwamba et al., 2016).

208 Overall, the subcellular distribution of Pb in both roots and shoots indicates that lettuce may be actively  
209 restricting the accumulation of Pb in nuclei and organelles as a protective mechanism. This mechanism, however,  
210 was shown to exist under Cu stress in the roots of lettuce, but not in shoots. There may be a delay in the Cu stress  
211 response of shoots when compared to roots. Thus, lettuce can activate its defense systems in time to counter the  
212 toxicity of Pb under severe PTE levels but is delayed in its defense against the toxicity of Cu. This results in higher  
213 mortality of lettuce seeds under severe Cu levels when compared with Pb. This might be the reason that the  
214 positive effect on yield and leaf chlorophyll occurs over a wider range of Pb concentrations than Cu concentrations  
215 (see regions “I–IV” in Fig. 1).

#### 216 4.4. Visualized distribution of Pb and Cu in lettuce, toxicity, and transport mechanisms

217 The distribution of Pb was significantly correlated with Ca in lettuce seeds (correlation coefficient, 0.624\*\*)   
218 under Pb stress (Table S5), indicating that the transport of Pb might be closely related to Ca in lettuce since Ca<sup>2+</sup>-  
219 permeable channels (a passive transport) is a primary pathway of Pb uptake (Trakal et al., 2015). The distribution  
220 of Cu was significantly correlated with Fe, Zn, and Mn both in seeds and seedling shoots under Cu stress. A major

221 reason for this might be that these elements are essential elements and all use similar active and passive transport  
222 systems during uptake (Trakal et al., 2013, 2015), despite the competition exists among the uptake of Cu and Fe,  
223 Zn, and Mn by plants.

224 Based on the  $\mu$ -XRF data of lettuce seeds (see Figs. 4 and 5), it was assumed that the mortality of lettuce seeds  
225 was primarily caused by the high accumulation of Pb and Cu in the radicle, resulting in cessation of radicle  
226 germination via damage to the cell division process from severe oxidative stress (Lamb et al., 2010). Previous  
227 studies have confirmed that high Pb and Cu stress impairs microtubule arrangements, damages DNA, and causes  
228 chromosomal aberrations of cells in the roots of corn and onion (Qin et al., 2015; Sun and Luo, 2018).

229 A large number of  $\text{Cu}^{2+}$  ions can be reduced to  $\text{Cu}^+$  in cells under high Cu stress, since cells are capable of  
230 catalyzing the formation of hydroxyl radicals ( $\text{OH}\cdot$ ) to initiate oxidative damage (Gaetke and Chow, 2003).  
231 Although copper chaperones sequester Cu in a non-reactive form (Himelblau and Amasino, 2000), free Cu ions  
232 readily oxidize thiol bonds within proteins. This causes a disruption of their structure when Cu exceeds a threshold  
233 value in plants (Briat and Lebrun, 1999). Lead oxidative stress (near  $300 \text{ mg L}^{-1}$ ) may also induce membrane  
234 damage to the cells of plants by producing excess ROS (Venkatachalam et al., 2017). Excess ROS can cause  
235 oxidative cell damage and even necrosis in plants due to the interaction of PTE ions with biomolecules (Yin et al.,  
236 2008). In conclusion, the toxicity of high concentrations of Pb and Cu to the radicles of lettuce seeds during  
237 germination is fatal.

238 Copper could be transported rapidly throughout the entire seed using both active and passive transport systems  
239 since Cu is an essential element for plants (Trakal et al., 2013). We discovered that the radicles of dead seeds  
240 under severe Cu levels extended noticeably out of the seed bodies (Fig. 5). Moreover, the mineral nutrients (e.g.,  
241 K, Ca, Fe, Mn, Cu, and Zn) involved in the metabolism of lettuce seed germination are preferentially and rapidly  
242 transported to the tip of the radicle and the tip of the cotyledon (Fig. 5), where metabolism is vigorous at levels

243 below the point of mortality. The radicles of dead seeds under severe Pb levels, however, barely protruded out of  
244 the seeds, while Pb, Fe, Mn, and Zn were only concentrated in the radicles of lettuce seeds (Fig. 4). We hypothesize  
245 that cells in lettuce seeds are more sensitive to the toxicity of Pb than Cu. In this scenario, the lettuce seeds died  
246 quickly under severe Pb levels, and there was not enough time to transport the mineral nutrient elements to the  
247 top of cotyledons, despite the fact that Fe, Mn, and Zn uptake uses active transport systems. The lettuce seeds died  
248 slowly under severe Cu levels, however, and there was enough time to germinate a radicle and transport mineral  
249 nutrients to the top of cotyledons. To our knowledge, this is the first report of spatial information on the migration  
250 and accumulation of PTEs and mineral elements in lettuce seeds.

251 Abundant amounts of iron and manganese accumulated in the root hair zone (region “f” in Fig. 7b), an  
252 occurrence that may be related to the formation of iron plaques on the root surface of lettuce seedlings. Iron plaque  
253 easily forms on the root surface of wetland plants (Tai et al., 2018), and can significantly affect the sorption and  
254 immobilization of PTEs in the soil-plant system, even during the seedling period (Li et al., 2020). The distributions  
255 of Pb and Cu were clearly collocated with Fe/Mn plaques in the root hair zone, primarily due to the chelation of  
256 Pb and Cu.

257 Transmission electron microscopy (TEM) is a powerful method for exploring the intuitive mechanism of PTE  
258 toxicity to organelles in plant cells (Sun and Luo, 2018). In future studies of the PTE toxicity mechanisms in  
259 plants, we can use TEM, synchrotron radiation-based Fourier transform infrared (SR-FTIR), and XAFS  
260 spectroscopy to identify PTE species and their binding structures with sorption sites in plant tissues.

## 261 **5. Conclusions**

262 This study demonstrated that lettuce plants use vacuoles and cell walls to reduce the transport of Pb and Cu  
263 through their roots as a protective mechanism. High accumulations of Pb and Cu in the radicle result in the death  
264 of lettuce seeds under severe levels of PTEs, while radicle growth of lettuce seed was easier inhibited by Pb at

265 severe levels than Cu. The PTE-loaded capacity that ensures food safety of Pb ( $65.1 \text{ mg kg}^{-1}$ ) in studied soil for  
266 lettuce was lower than that of Cu ( $89.9 \text{ mg kg}^{-1}$ ), whereas the PTE-loaded capacity that limits yield and the PTE-  
267 loaded capacity that kills seeds of Pb ( $997.2$  and  $2643.5 \text{ mg kg}^{-1}$ ) were much higher than those of Cu ( $212.1$  and  
268  $525.4 \text{ mg kg}^{-1}$ ). The health risk of Pb in visually healthy lettuce appeared to be higher than that of Cu under the  
269 same soil contamination level. We strongly recommend a strengthened food safety supervision and inspection in  
270 agricultural production to reduce the health risk of PTEs via visually healthy vegetables (with excessive PTEs  
271 content, however) intake.

272

### 273 **Declaration of Competing Interest**

274 The authors declare that they have no known competing financial interests or personal relationships that could  
275 have appeared to influence the work reported in this paper.

### 276 **Acknowledgments**

277 The  $\mu$ -XRF beam time was granted by 4W1B beamline of Beijing Synchrotron Radiation Facility, Institute of  
278 High Energy Physics (Chinese Academy of Sciences). We are indebted to all staff members of 4W1B for their  
279 support in measurements and data reduction. This work was financially supported by the National Key Research  
280 and Development Program of China (2017YFD0202101), the National Natural Science Foundation of China  
281 (21866013, 21876027, 51904079), the United Fund of Guangdong Provincial Basic and Applied Basic Research  
282 Foundation, China (2019A1515110705), the Crop Science Postgraduate Innovation Project of Hainan University  
283 Tropical Agriculture and Forestry College (ZWCX2018012, ZWCX2018013), the Ministry of Education, Youth  
284 and Sports of the Czech Republic (CZ.02.1.01/0.0/0.0/16\_026/0008403), and the Special Funding for the Science  
285 and Technology Innovation Team of Foshan, China (1920001000083).

286

287 **References**

- 288 Ali, S., Chaudhary, A., Rizwan, M., Anwar, H.T., Adrees, M., Farid, M., Irshad, M.K., Hayat, T., Anjum, S.A., 2015.
- 289 Alleviation of chromium toxicity by glycinebetaine is related to elevated antioxidant enzymes and suppressed chromium
- 290 uptake and oxidative stress in wheat (*Triticum aestivum* L.). *Environ. Sci. Pollut. Res.* 22, 10669–10678.
- 291 <https://doi.org/10.1007/s11356-015-4193-4>
- 292 Bandara, T., Franks, A., Xu, J., Bolan, N., Wang, H., Tang, C., 2020. Chemical and biological immobilization mechanisms of
- 293 potentially toxic elements in biochar-amended soils. *Crit. Rev. Environ. Sci. Technol.* 50, 903–978.
- 294 <https://doi.org/10.1080/10643389.2019.1642832>
- 295 Bao, S., 2000. *Chemical Analysis for Agricultural Soil*. China Agriculture Press, Beijing.
- 296 Briat, J.F., Lebrun, M., 1999. Plant responses to metal toxicity. *Comp. R. Acad. Sci. Paris.* 322, 43–54.
- 297 [https://doi.org/10.1016/S0764-4469\(99\)80016-X](https://doi.org/10.1016/S0764-4469(99)80016-X)
- 298 Cai, L.M., Wang, Q.S., Luo, J., Chen, L.G., Zhu, R.L., Wang, S., Tang, C.H., 2019. Heavy metal contamination and health risk
- 299 assessment for children near a large Cu-smelter in Central China. *Sci. Total. Environ.* 650, 725–733.
- 300 <https://doi.org/10.1016/j.scitotenv.2018.09.081>
- 301 Calabrese, E.J., 2008. Hormesis: why it is important to toxicology and toxicologists. *Environ. Toxicol. Chem.* 27(7), 1451–
- 302 1474. <https://doi.org/10.1897/07-541>
- 303 Chen, H., Yang, X., Wang, H., Sarkar, B., Shaheen, S.M., Gielen, G., Bolan, N., Guo, J., Che, L., Sun, H., Rinklebe, J., 2020.
- 304 Animal carcass- and wood-derived biochars improved nutrient bioavailability, enzyme activity, and plant growth in metal-
- 305 phthalic acid ester co-contaminated soils: A trial for reclamation and improvement of degraded soils. *J. Environ. Manage.*
- 306 261(1), 110246. <https://doi.org/10.1016/j.jenvman.2020.110246>
- 307 Cobb, G.P., Sands, K., Waters, M., Wixson, B.G., Dorward-King, E., 2000. Accumulation of heavy metals by vegetables grown
- 308 in mine wastes. *Environ. Toxicol. Chem.* 19, 600–607. <https://doi.org/10.1002/etc.5620190311>

309 DEFRA and Environment Agency, 2002. Contaminations in soil: collation of toxicological data and intake values for humans,  
310 Publication CLR9. The R&D Dissemination Centre, WRC plc, Swindon, Wilts.

311 Ding, C.F., Li, X.G., Zhang, T.L., Wang, X.X., 2015. Transfer model of lead in soil-carrot (*Daucus carota* L.) system and food  
312 safety thresholds in soil. *Environ. Toxicol. Chem.* 34(9), 2078–2086. <https://doi.org/10.1002/etc.3031>

313 Dong, Y.X., Wang, X.F., Cui, X.M. 2013. Exogenous nitric oxide involved in subcellular distribution and chemical forms of  
314  $\text{Cu}^{2+}$  under copper stress in tomato seedlings. *J. Integr. Agr.* 12(10), 1783–1790. [https://doi.org/10.1016/S2095-3119\(13\)60367-6](https://doi.org/10.1016/S2095-3119(13)60367-6)

315

316 Fang, Z., Gao, Y., Bolan, N., Shaheen, S.M., Xu, S., Wu, X., Xu, X., Hu, H., Lin, J., Zhang, F., Li, J., Rinklebe, J., Wang, H.,  
317 2020. Conversion of biological solid waste to graphene-containing biochar for water remediation: A critical review. *Chem.*  
318 *Eng. J.* 390, 124611. <https://doi.org/10.1016/j.cej.2020.124611>

319 FAOSTAT (UN Food & Agriculture Organization, Statistics Division) Lettuce (with chicory) area harvested in 2018, 2019.  
320 Retrieved March 4, 2020. <http://www.fao.org/faostat/en/#data/QC>

321 Ferri, R., Hashim, D., Smith, D.R., Guazzetti, S., Donna, F., Ferretti, E., Curatolo, M., Moneta, C., Beone, G.M., Lucchini,  
322 R.G., 2015. Metal contamination of home garden soils and cultivated vegetables in the province of Brescia, Italy:  
323 implications for human exposure. *Sci. Total. Environ.* 518–519, 507–517.  
324 <https://doi.org/10.1016/j.scitotenv.2015.02.072>

325 Gaetke, L.M., Chow, C.K., 2003. Copper toxicity, oxidative stress, and antioxidant nutrients. *Toxicology* 189(1–2), 147–163.  
326 [https://doi.org/10.1016/S0300-483X\(03\)00159-8](https://doi.org/10.1016/S0300-483X(03)00159-8)

327 Gomes, M.P., Duarte, D.M., Carneiro, M.M.L.C., Barreto, L.C., Carvalho, M., Soares, A.M., Guilherme, L.R., Garcia, Q.S.,  
328 2013. Zinc tolerance modulation in *Myracrodruon urundeuva* plants. *Plant. Physiol. Bioch.* 67, 1–6.  
329 <https://doi.org/10.1016/j.plaphy.2013.02.018>

330 Gruszecka-Kosowska, A., 2019. Potentially Harmful Element Concentrations in the Vegetables Cultivated on Arable Soils,

331 with Human Health-Risk Implications. *Int. J. Environ. Res. Public Health*. 16, 4053.  
332 <https://doi.org/10.3390/ijerph16204053>

333 Himelblau, E., Amasino, R.M., 2000. Delivering copper within plant cells. *Curr. Opin. Plant. Biol.* 3, 205–210.  
334 [https://doi.org/10.1016/S1369-5266\(00\)80066-7](https://doi.org/10.1016/S1369-5266(00)80066-7)

335 Hou, S., Zheng, N., Tang, L., Ji, X., 2018. Effects of cadmium and copper mixtures to carrot and pakchoi under greenhouse  
336 cultivation condition. *Ecotoxicol. Environ. Saf.* 159, 172–181. <https://doi.org/10.1016/j.ecoenv.2018.04.060>

337 ISO, 1995. Soil quality—determination of the effects of pollutants on soil flora—part 2: effects of chemicals on the emergence  
338 of higher plants. ISO—International organization for standardization Genève, pp 2–7.

339 Kabata-Pendias, A., 2011. Trace elements in soils and plants. CRC/Taylor and Francis Group, Boca Raton, FL.

340 Kim, M.J., Moon, Y., Tou, J.C., Mou, B., Waterland, N.L., 2016. Nutritional value, bioactive compounds and health benefits  
341 of lettuce (*Lactuca sativa* L.). *J. Food. Compos. Anal.* 49, 19–34. <https://doi.org/10.1016/j.jfca.2016.03.004>

342 Lamb, D.T., Ming, H., Megharaj, M., Naidu, R., 2010. Relative tolerance of a range of Australian native plant species and  
343 lettuce to copper, zinc, cadmium, and lead. *Arch. Environ. Con. Tox.* 59(3), 424–432. [https://doi.org/10.1007/s00244-](https://doi.org/10.1007/s00244-010-9481-x)  
344 [010-9481-x](https://doi.org/10.1007/s00244-010-9481-x)

345 Li, J., Wang, S-L., Zhang, J., Zheng, L., Chen, D., Wu, Z., Shaheen, S.M., Rinklebe, J., Ok, Y.S., Wang, H., Wu, W., 2020.  
346 Coconut-fiber biochar reduced the bioavailability of lead but increased its translocation rate in rice plants: Elucidation of  
347 immobilization mechanisms and significance of iron plaque barrier on roots using spectroscopic techniques. *J. Hazard.*  
348 *Mater.* 389, 122117. <https://doi.org/10.1016/j.jhazmat.2020.122117>

349 Li, J., Wang, S-L., Zheng, L., Chen, D., Wu, Z., Xie, Y., Wu, W., Niazi, N.K., Ok, Y.S., Rinklebe, J., Wang, H. 2019a. Sorption  
350 of lead in soil amended with coconut fiber biochar: Geochemical and spectroscopic investigations. *Geoderma*. 350, 52–  
351 60. <https://doi.org/10.1016/j.geoderma.2019.05.008>

352 Li, J., Zheng, L., Wang, S-L., Wu, Z., Wu, W., Niazi, N.K., Shaheen, S.M., Rinklebe, J., Bolan, N., Ok, Y.S., Wang, H., 2019b.



353 Sorption mechanisms of lead on silicon-rich biochar in aqueous solution: Spectroscopic investigation. *Sci. Total. Environ.*  
354 672, 572–582. <https://doi.org/10.1016/j.scitotenv.2019.04.003>

355 Liu, B., Ai, S., Zhang, W., Huang, D., Zhang, Y., 2017. Assessment of the bioavailability, bioaccessibility and transfer of heavy  
356 metals in the soil-grain-human systems near a mining and smelting area in NW China. *Sci. Total. Environ.* 609, 822–829.  
357 <https://doi.org/10.1016/j.scitotenv.2017.07.215>

358 Lu, K., Yang, X., Gielen, G., Bolan, N., Ok, Y.S., Niazi, N.K., Xu, S., Yuan, G., Chen, X., Zhang, X., Liu, D., Song, Z., Liu,  
359 X., Wang, H., 2017a. Effect of bamboo and rice straw biochars on the mobility and redistribution of heavy metals (Cd,  
360 Cu, Pb and Zn) in contaminated soil. *J. Environ. Manage.* 186, 285–292. <https://doi.org/10.1016/j.jenvman.2016.05.068>

361 Lu, L., Xie, R., Liu, T., Wang, H., Hou, D., Du, Y., He, Z., Yang, X., Sun, H., Tian, S., 2017b. Spatial imaging and speciation  
362 of Cu in rice (*Oryza sativa* L.) roots using synchrotron-based X-ray microfluorescence and X-ray absorption spectroscopy.  
363 *Chemosphere* 175, 356–364. <https://doi.org/10.1016/j.chemosphere.2017.02.082>

364 Mackay, A.K., Taylor, M.P., Munksgaard, N.C., Hudson-Edwards, K.A., Burn-Nunes, L., 2013. Identification of environmental  
365 lead sources and pathways in a mining and smelting town: Mount Isa, Australia. *Environ. Pollut.* 180, 304–311.  
366 <https://doi.org/10.1016/j.envpol.2013.05.007>

367 Megateli, S., Semsari, S., Couderchet, M. 2009. Toxicity and removal of heavy metals (cadmium, copper, and zinc) by *Lemna*  
368 *gibba*. *Ecotox. Environ. Safe.* 72, 1774–1780. <https://doi.org/10.1016/j.ecoenv.2009.05.004>

369 Mwamba, T.M., Li, L., Gill, R.A., Islam, F., Nawaz, A., Ali, B., Farooq, M.A., Lwalaba, J.L., Zhou, W., 2016. Differential  
370 subcellular distribution and chemical forms of cadmium and copper in *Brassica napus*. *Ecotox. Environ. Safe.* 134,  
371 239–249. <https://doi.org/10.1016/j.ecoenv.2016.08.021>

372 NAAS (National Agricultural Advisory Service) Crop Values 2014 Summary, 2015. United States Department of Agriculture.  
373 <http://www.usda.gov/nass/PUBS/TODAYRPT/cpvl0215.pdf>

374 Qin, R., Wang, C., Chen, D., Björn, L.O., Li, S. 2015. Copper-induced root growth inhibition of *Allium cepa* *Var. agrogarum*

375 L. involves disturbances in cell division and DNA damage. *Environ. Toxicol. Chem.* 34(5), 1045–1055.  
376 <https://doi.org/10.1002/etc.2884>

377 Rayment, G.E., Higginson, F.R., 1992. *Australian Laboratory Handbook of Soil and Water Chemical Methods*, Inkata,  
378 Melbourne.

379 Setia, R.C., Kaur, N., Setia, N., Nayyar, H., 2018. Heavy Metal Toxicity in Plants and Phytoremediation. In *Crop Improvement: Strategies and Applications*.  
380

381 Shahid, M., Shamshad, S., Rafiq, M., Khalid, S., Bibi, I., Niazi, N.K., Dumat, C., Rashid, M.I., 2017. Chromium speciation,  
382 bioavailability, uptake, toxicity and detoxification in soil-plant system: a review. *Chemosphere* 178, 513–533.  
383 <https://doi.org/10.1016/j.chemosphere.2017.03.074>

384 Shahid, M., Niazi, N.K., Rinklebe, J., Bundschuh, J., Dumat, C., Pinelli, E., 2019. Trace elements-induced phytohormesis: A  
385 critical review and mechanistic interpretation. *Crit. Rev. Environ. Sci. Technol.*  
386 <https://doi.org/10.1080/10643389.2019.1689061>

387 Shu, X., Yin, L., Zhang, Q., Wang, W., 2012. Effect of Pb toxicity on leaf growth, antioxidant enzyme activities, and  
388 photosynthesis in cuttings and seedlings of *Jatropha curcas* L. *Environ. Sci. Pollut. Res.* 19(3), 893–902.  
389 <https://doi.org/10.1007/s11356-011-0625-y>

390 Sokolova, I., Ringwood, A., Johnson, C., 2005. Tissue-specific accumulation of cadmium in subcellular compartments of  
391 eastern oysters *Crassostrea virginica* Gmelin (Bivalvia: Ostreidae). *Aquat. Toxicol.* 74(3), 218–228.  
392 <https://doi.org/10.1016/j.aquatox.2005.05.012>

393 Solé, V.A., Papillon, E., Cotte, M., Walter, P., Susini, J., 2007. A multiplatform code for the analysis of energy-dispersive X-  
394 ray fluorescence spectra. *Spectrochim. Acta. Part B* 62, 63–68. <https://doi.org/10.1016/j.sab.2006.12.002>

395 Sun, J., Luo, L., 2018. Subcellular distribution and chemical forms of Pb in corn: strategies underlying tolerance in Pb stress. *J. Agr. Food. Chem.* 66, 6675–6682. <https://doi.org/10.1021/acs.jafc.7b03605>  
396

397 Tai, Y., Tam, N.F., Wang, R., Yang, Y., Lin, J., Wang, J., Yang, Y., Li, L., Sun, Y., 2018. Iron plaque formation on wetland-plant  
398 roots accelerates removal of water-borne antibiotics. *Plant Soil* 433, 323–338. <https://doi.org/10.1007/s11104-018-3843->  
399 [y](https://doi.org/10.1007/s11104-018-3843-y)

400 Trakal, L., Kodešová, R., Komárek, M., 2013. Modelling of Cd, Cu, Pb and Zn transport in metal contaminated soil and their  
401 uptake by willow (*Salix × smithiana*) using HYDRUS-2D program. *Plant Soil* 366, 433–451.  
402 <https://doi.org/10.1007/s11104-012-1426-x>

403 Trakal, L., Martínez-Fernández, D., Vítková, M., Komárek, M., 2015. Phytoextraction of Metals: Modeling Root Metal Uptake  
404 and Associated Processes. In *Phytoremediation: Management of Environmental Contaminants* 1, 69–83.  
405 [https://doi.org/10.1007/978-3-319-10395-2\\_6](https://doi.org/10.1007/978-3-319-10395-2_6)

406 van Assche, F., Clijsters, H., 1990. Effects of metals on enzyme activity in plants. *Plant Cell Environ.* 13, 195–206.  
407 <https://doi.org/10.1111/j.1365-3040.1990.tb01304.x>

408 Venkatachalam, P., Jayalakshmi, N., Geetha, N., Sahi, S.V., Sharma, N.C., Rene, E.R., Sarkar, S.K., Favas, P.J.C., 2017.  
409 Accumulation efficiency, genotoxicity and antioxidant defense mechanisms in medicinal plant *Acalypha indica* L. under  
410 lead stress. *Chemosphere* 171, 544–553. <https://doi.org/10.1016/j.chemosphere.2016.12.092>

411 Webb, B., Adeloju, S.B., 2013. Evaluation of some wet digestions methods for reliable determination of total phosphorus in  
412 Australian soils. *Microchem. J.* 111(14), 47–52. <https://doi.org/10.1016/j.microc.2013.02.001>

413 Wenzel, W.W., 2009. Rhizosphere processes and management in plant-assisted bioremediation (phytoremediation) of  
414 soils. *Plant Soil* 321, 385–408. <https://doi.org/10.1007/s11104-008-9686-1>

415 Wu, W., Li, J., Lan, T., Müller, K., Niazi, N.K., Chen, X., Xu, S., Zheng, L., Chu, Y., Li, J., Yuan, G., Wang, H., 2017.  
416 Unraveling sorption of lead in aqueous solutions by chemically modified biochar derived from coconut fiber: A  
417 microscopic and spectroscopic investigation. *Sci. Total. Environ.* 576, 766–774.  
418 <https://doi.org/10.1016/j.scitotenv.2016.10.163>

419 Wu, Z., McGrouther, K., Chen, D., Wu, W., Wang, H., 2013. Subcellular Distribution of Metals within *Brassica chinensis* L.  
420 in Response to Elevated Lead and Chromium Stress. *J. Agr. Food. Chem.* 61, 4715–4722.  
421 <https://doi.org/10.1021/jf4005725>

422 Wu, Z., Mcgrouther, K., Huang, J., Wu, P., Wu, W., Wang, H., 2014. Decomposition and the contribution of glomalin-related  
423 soil protein (GRSP) in heavy metal sequestration: field experiment. *Soil Biology. Biochem.* 68(1), 283–290.  
424 <https://doi.org/10.1016/j.soilbio.2013.10.010>

425 Xia, S., Song, Z., Jeyakumar, P., Bolan, N., Wang, H., 2020. Characteristics and applications of biochar for remediating Cr(VI)-  
426 contaminated soils and wastewater. *Environ. Geochem. Hlth.* <https://doi.org/10.1007/s10653-019-00445-w>

427 Yang, D., Guo, Z., Green, I.D., Xie, D., 2016. Effect of cadmium accumulation on mineral nutrient levels in vegetable crops:  
428 potential implications for human health. *Environ. Sci. Pollution. Res.* 23(19), 19744–19753. <https://doi.org/10.1007/s11356-016-7186-z>

429

430 Yin, X.L., Jiang, L., Song, N.K., Yang, H., 2008. Toxic reactivity of wheat (*Triticum aestivum*) plants to herbicide isoproturon.  
431 *J. Agr. Food. Chem.* 56, 4825–4831. <https://doi.org/10.1021/jf800795v>

432 Yuan, Y., Xiang, M., Liu, C., Theng, B.K.G., 2019. Chronic impact of an accidental wastewater spill from a smelter, China: A  
433 study of health risk of heavy metal(loid)s via vegetable intake. *Ecotox. Environ. Safe.* 182, 109401.  
434 <https://doi.org/10.1016/j.ecoenv.2019.109401>

435 Zhang, C., Zhang, P., Mo, C., Yang, W., Li, Q., Pan, L., Lee, D.K., 2013. Cadmium uptake, chemical forms, subcellular  
436 distribution, and accumulation in *Echinodorus osiris* Rataj. *Environ. Sci-Proc. Imp.* 15(7), 1459–1465.  
437 <https://doi.org/10.1039/c3em00002h>

438

439 **Table 1**440 Lead and copper concentrations (mg kg<sup>-1</sup>, DW) in the shoots and roots of lettuce

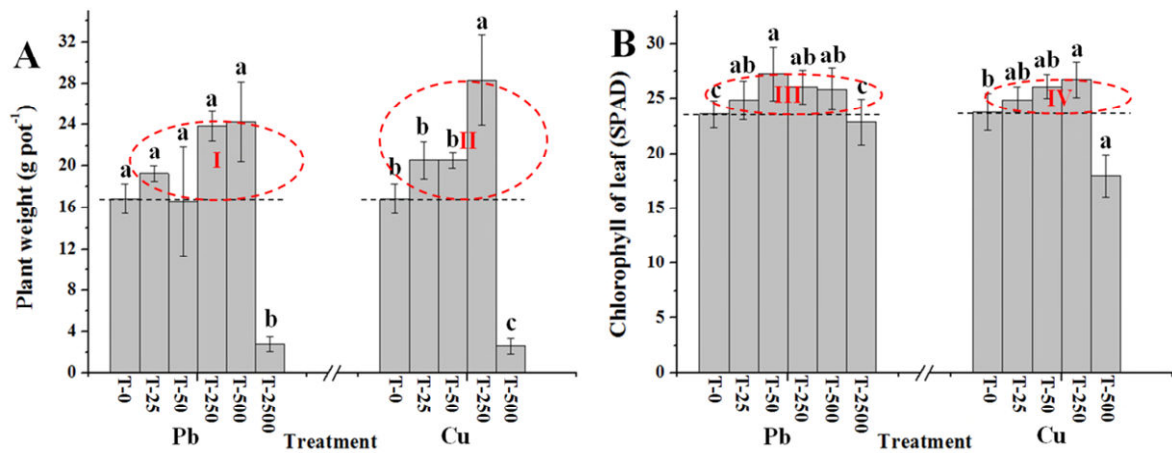
PTE level	Pb treatment			Cu treatment		
	Shoot	Root	TF (%)	Shoot	Root	TF (%)
0	5.73 ± 0.34d	17.4 ± 0.87d	33.1 ± 3.6a	78.0 ± 5.85d	118.8 ± 4.1d	65.5 ± 2.7a
25	9.76 ± 0.49d	35.7 ± 2.14d	27.3 ± 1.5b	152.2 ± 17.5c	338.1 ± 20.5c	44.9 ± 2.4b
50	56.3 ± 4.51c	201.4 ± 16.1c	28.2 ± 4.1ab	203.4 ± 13.6b	685.2 ± 19.9b	29.7 ± 1.1c
250	210.9 ± 19.0b	892.7 ± 64.5b	23.6 ± 0.5b	299.9 ± 23.0a	2353 ± 81.6a	12.7 ± 0.5d
500	432.7 ± 21.6a	1789 ± 89.5a	24.3 ± 2.4b	--	--	--

441 Notes: Results are means ± SD; DW refers to dry weight. The translocation factor (TF) was used to evaluate the

442 ability of plants to translocate Pb or Cu from the roots to the shoots using the following equation:  $TF = 100 \times$ 443  $C_{\text{shoot}}/C_{\text{root}}$ , where C refers to the concentration of potentially toxic element (PTE) in tissues (mg kg<sup>-1</sup> DW). Values444 within a column followed by the same letter do not differ significantly (Tukey's multiple-range test,  $p = 0.05$ ; number of

445 replications per treatment = 3).

446



447

448 **Fig. 1** (A) Weight of lettuce (*Lactuca sativa* L.) plants and (B) chlorophyll content of lettuce leaves in studied soils with

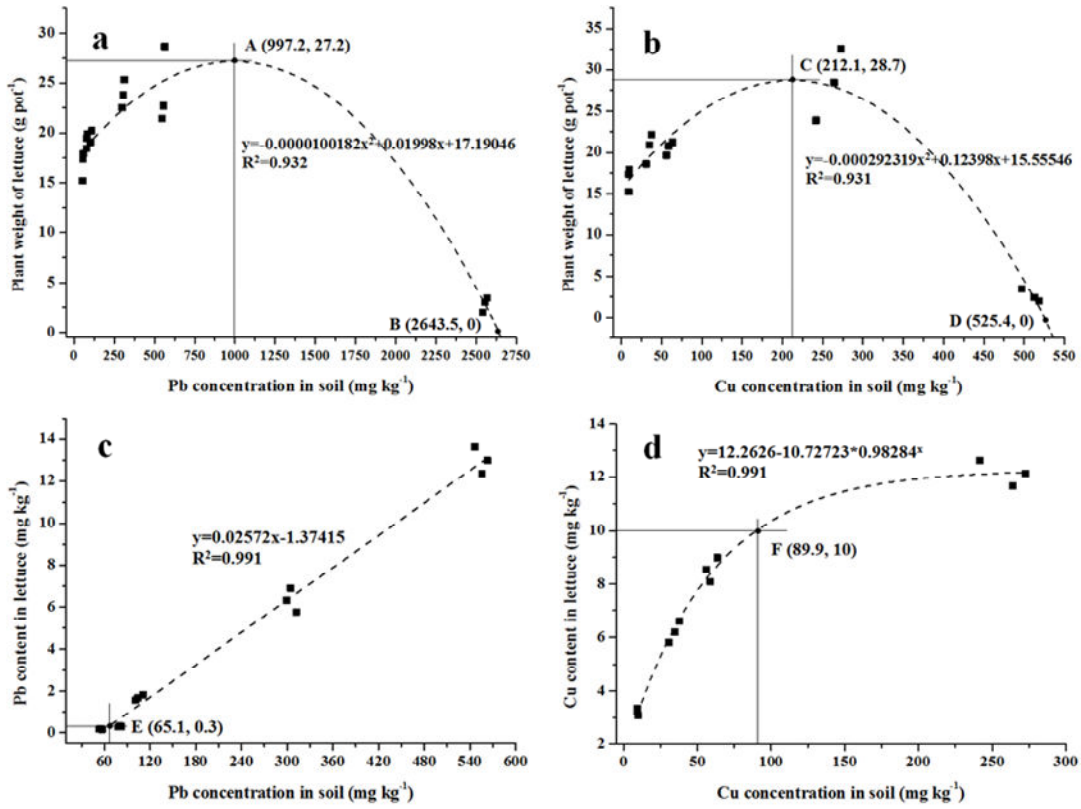
449 different Pb and Cu levels; regions “I,” “II,” “III,” and “IV” indicate the area between the value of the control treatment and

450 the highest value, i.e., the homeotic effect zone. The T-0, T-25, T-50, T-250, T-500, and T-2500 labels refer to contaminated PTE

451 levels of 0, 25, 50, 250, 500, and 2500 mg kg<sup>-1</sup> in soils, respectively. Different lowercase letters on the bar graph indicate

452 significant differences between treatments ( $p < 0.05$ ).

453



454

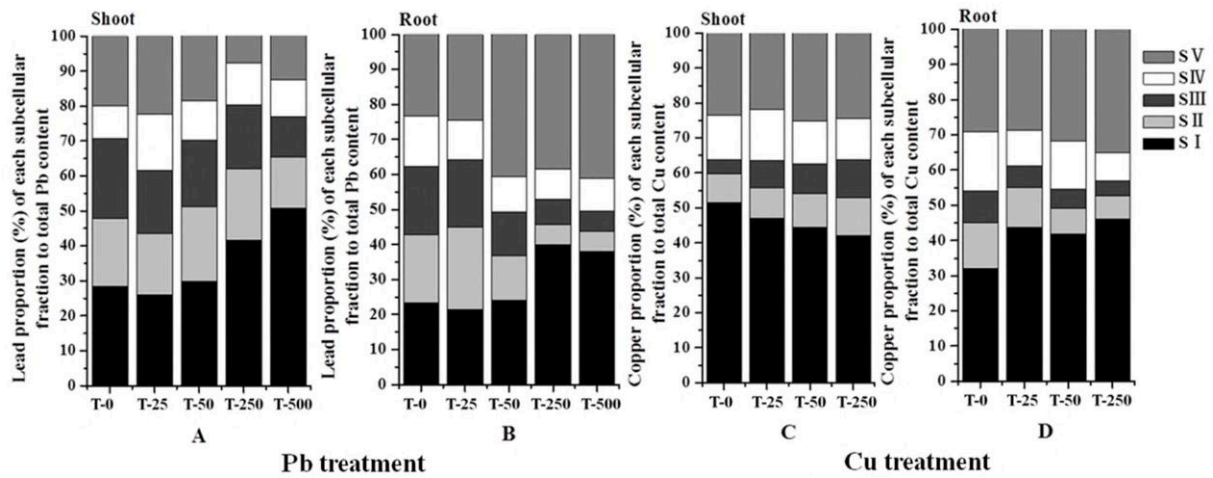
455 **Fig. 2** (a–b) Lettuce plant weight with increasing Pb and Cu levels in contaminated soil, A and B show the yield decreasing

456 concentration and lethal concentration of Pb for lettuce, while C and D show the yield decreasing concentration and lethal

457 concentration of Cu for lettuce. (c–d) The PTE content in lettuce with increasing Pb and Cu concentrations in contaminated

458 soil, E and F show the safety concentrations of Pb and Cu for lettuce.

459



460

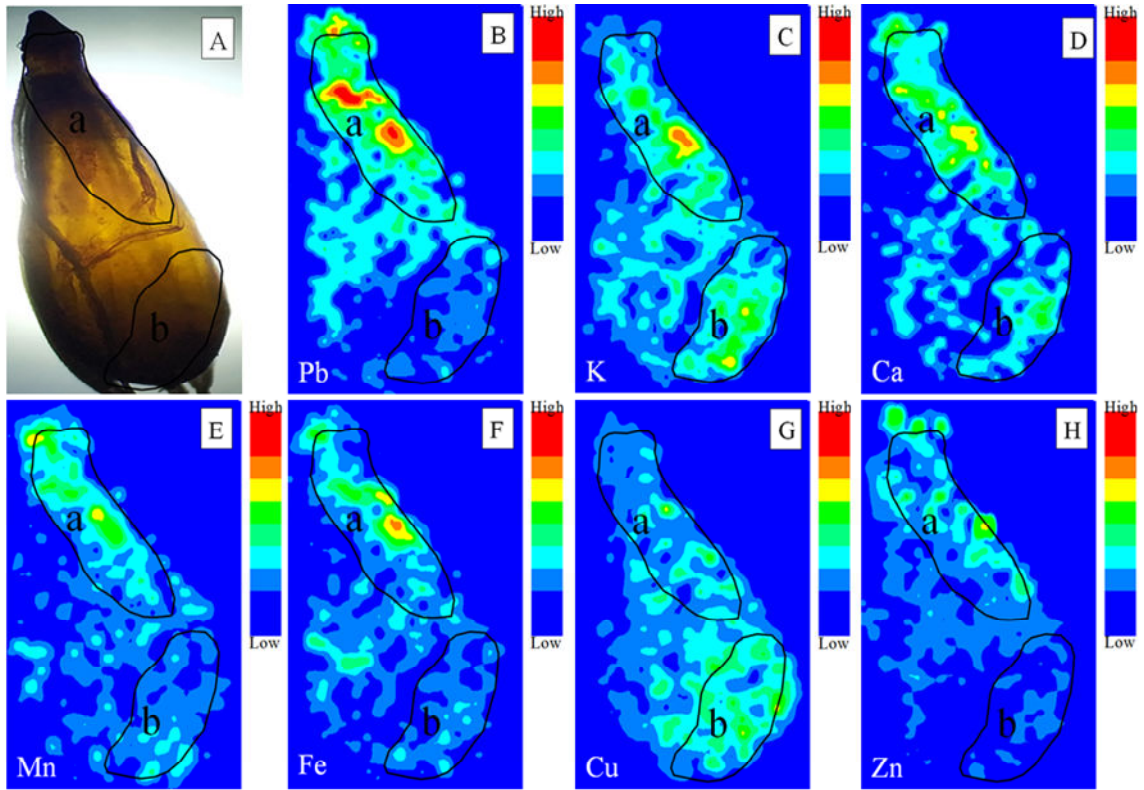
461 **Fig. 3** Subcellular proportions of Pb (A and B) and Cu (C and D) in shoots and roots of lettuce plants under different Pb and

462 Cu levels; SI, SII, SIII, SIV, and SV refer to the supernatant soluble fraction, mitochondrion, nucleus, plastid, and cell wall of

463 lettuce cells, respectively.

464





465

466

**Fig. 4** (A) photo and (B–H)  $\mu$ -XRF images of Pb, K, Ca, Mn, Fe, Cu, and Zn distributions in longitudinal sections of dead

467

lettuce seeds (poisoned to death) in response to Pb level of  $5000 \text{ mg kg}^{-1}$  in studied soil. These seeds were collected on the 5th

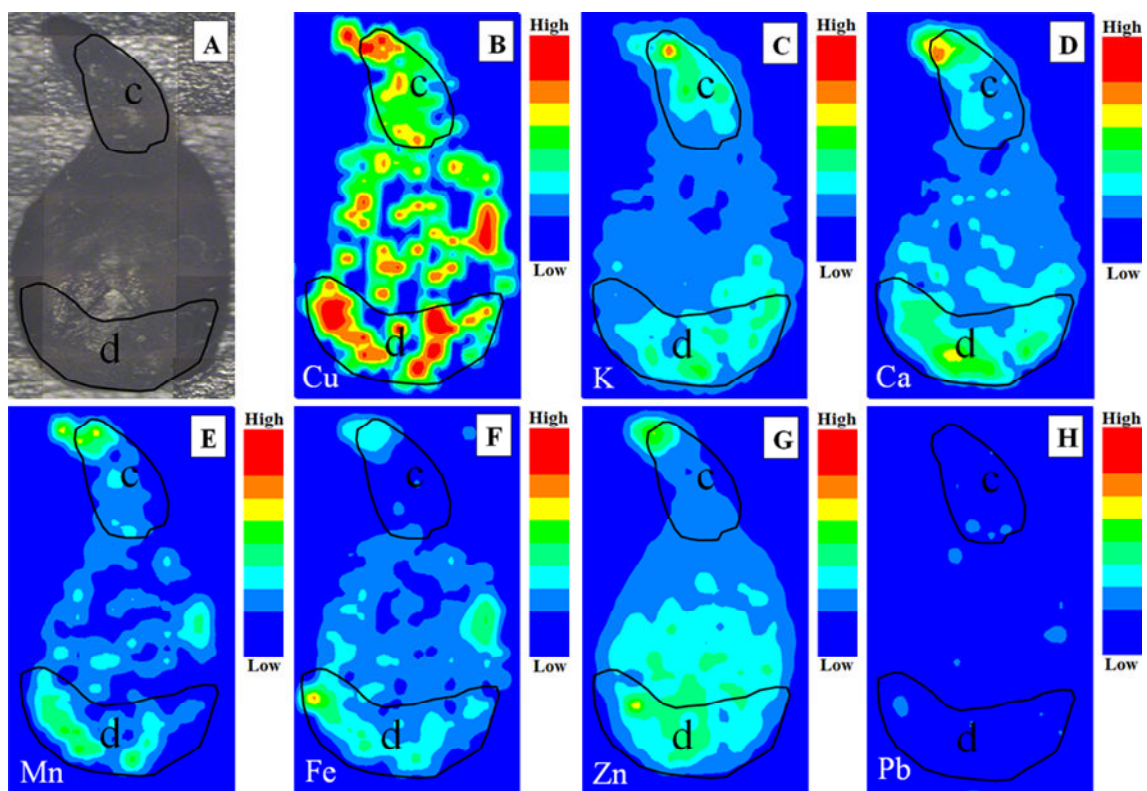
468

day after sowing. Lower fluorescence intensities (corresponding to lower concentrations) tend toward the blue end of the color

469

scale while higher intensities tend toward the red end of the color scale.

470



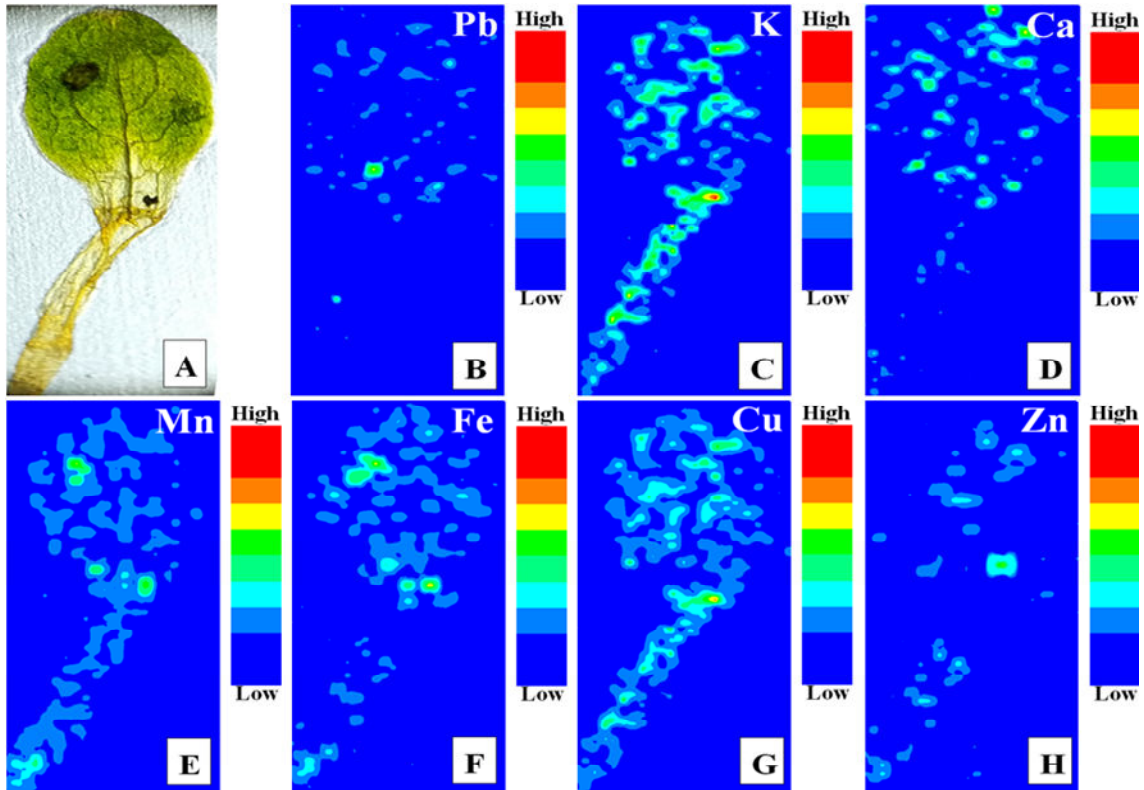
471

472 **Fig. 5** The  $\mu$ -XRF images of Cu, K, Ca, Mn, Fe, Zn, and Pb distribution in longitudinal sections of dead lettuce seeds (poisoned

473 to death) in response to a Cu level of  $2500 \text{ mg kg}^{-1}$  in studied soil. Samples were collected on the 5th day. Higher fluorescence

474 intensities tend toward the red end of the color scale while lower intensities tend toward the blue.

475



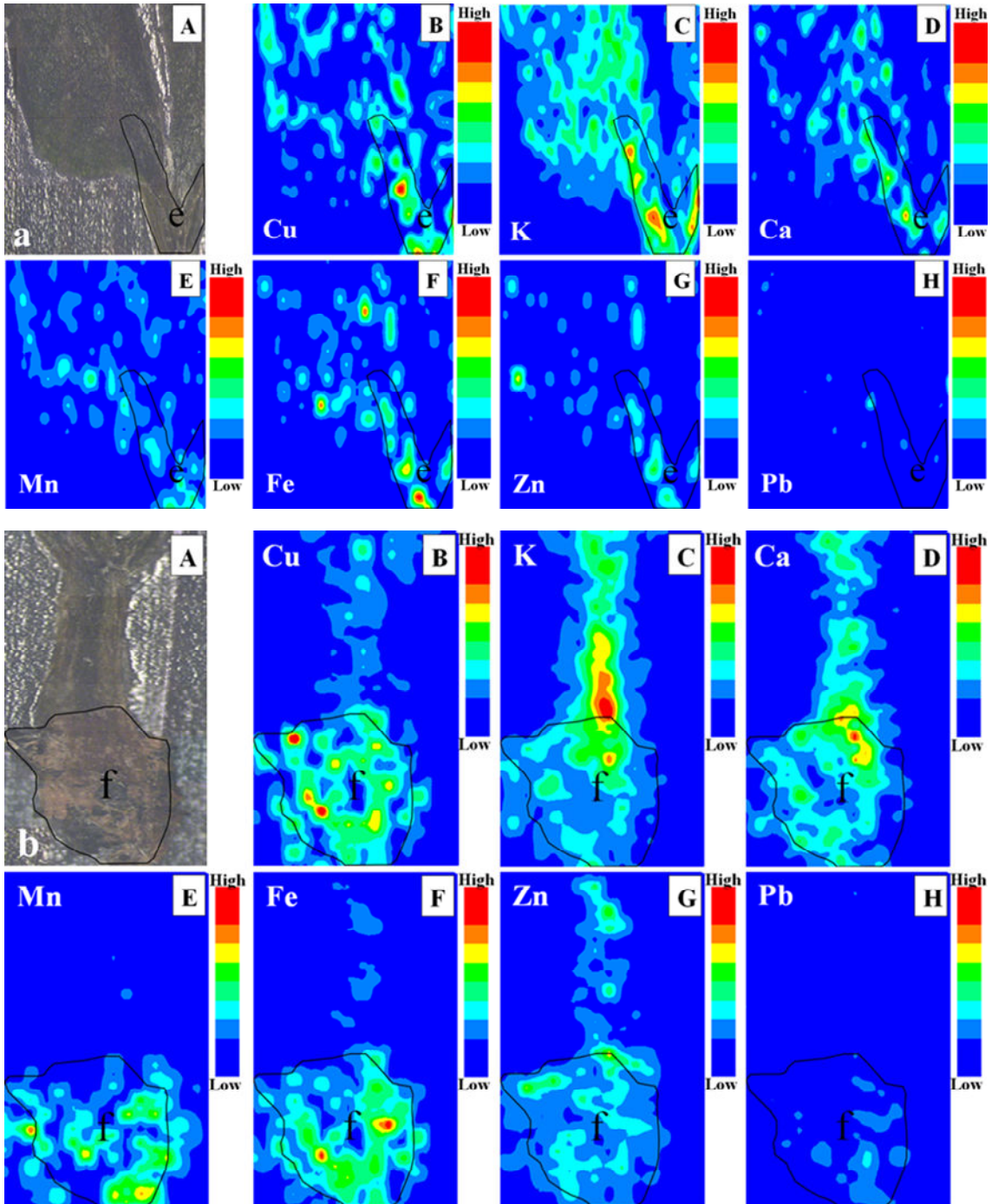
476

477 **Fig. 6** The  $\mu$ -XRF images of Pb, K, Ca, Mn, Fe, Cu, and Zn distribution in longitudinal sections of lettuce seedling in response

478 to a Pb level of  $50 \text{ mg kg}^{-1}$  in studied soil. Samples were collected on the 5th day. Lower fluorescence intensities tend toward

479 the blue end of the color scale while higher intensities tend toward the red end of the color scale.

480



481

482

483 **Fig. 7** The  $\mu$ -XRF images of Cu, K, Ca, Mn, Fe, Zn, and Pb distribution in longitudinal sections of lettuce seedling (a) shoots

484 and (b) roots in response to Cu levels of  $50 \text{ mg kg}^{-1}$  in studied soil. Samples were collected on the 5th day after sowing. Higher

485 fluorescence intensities (corresponding to higher concentrations) tend toward the red end of the color scale while lower

486 intensities tend toward the blue.